

Spin susceptibility of two-dimensional electrons in narrow AlAs quantum wells

K. Vakili, Y. P. Shkolnikov, E. Tutuc, E. P. De Poortere, and M. Shayegan
Department of Electrical Engineering, Princeton University, Princeton, NJ 08544
(dated: February 8, 2020)

We report measurements of the spin susceptibility in dilute two-dimensional electrons confined to a 45 Å wide AlAs quantum well. The electrons in this well occupy an out-of-plane conduction-band valley, rendering a system similar to two-dimensional electrons in Si MOSFETs but with only one valley occupied. We observe an enhancement of the spin susceptibility over the band value that increases as the density is decreased, following closely the prediction of quantum Monte Carlo calculations and continuing at finite values through the metal-insulator transition.

PACS numbers: 71.70.Ej, 73.43.Qt, 73.50.-h

As the density of a low-disorder two-dimensional electron system (2DES) is lowered, the Coulomb energy dominates over the kinetic (Fermi) energy and is expected to lead to a host of correlated states at low temperatures. According to quantum Monte Carlo (QMC) calculations, for example, the spin susceptibility χ/g^*m^* of the 2DES should rise and diverge below a critical density at which the system attains a ferromagnetic ground state (g^* and m^* are the renormalized Lande g -factor and mass respectively) [1]. Recent experiments [2, 3, 4, 5, 6, 7, 8, 9] in a number of different 2DESs have indeed revealed a rise in g^*m^* with decreasing density, and there is even a report of the divergence of g^*m^* at a density where the system exhibits a metal-insulator transition [4]. Almost none of the measurements, however, agree quantitatively with the results of QMC calculations. Moreover, in Si MOSFETs it is reported that the main contribution to the g^*m^* enhancement comes from an increase in m^* rather than g^* [10], also contrary to the QMC prediction.

We report here measurements of g^*m^* and m^* as a function of density in high-mobility 2DESs confined to very narrow AlAs quantum wells (QWs). In several respects, this is a nearly ideal system to study the properties of a dilute 2DES: it is a single-valley system with an isotropic in-plane Fermi contour and a thin electron layer. We find that g^*m^* in this system follows closely the prediction of recent QMC calculations [1]. The agreement continues through the metal-insulator transition, and we observe no corresponding ferromagnetic instability at that density. Our measurements of m^* exhibit a sample and cooldown dependence that betray a possible inadequacy of the Dingle analysis in this system.

Bulk AlAs has an indirect band-gap with the conduction-band minima at the six equivalent X -points of the Brillouin zone. The Fermi surface consists of six, anisotropic, half-ellipsoids (three full-ellipsoids or valleys), with transverse and longitudinal band masses of $m_t \approx 0.2$ and $m_l \approx 1$ respectively. This is similar to Si except that Si has six conduction-band valleys centered on points along the Δ -lines of the Brillouin zone. Electrons are confined along the growth (z) direction in a narrow (<

55 Å) AlAs QW occupy the single out-of-plane (X_z) valley since its higher m^* along z gives a lower confinement energy than for the in-plane (X_x, X_y) valleys [11, 12, 13]. This is again similar to the 2DES in Si MOSFETs fabricated on (001) Si substrates, except that in the Si case two valleys are occupied.

We performed measurements on four samples (A1, A2, A3, B1) from two different wafers (A and B). All were Si-modulation doped, 45 Å-wide, AlAs QWs with $\text{Al}_{0.4}\text{Ga}_{0.6}\text{As}$ barriers, grown on GaAs (001) substrates. We patterned the samples in a Hall bar configuration, and made ohmic contacts by depositing AuGeNi and alloying in a reducing environment. Metallic front and back gates were deposited to control the carrier density, n , which was determined from the frequency of Shubnikov-de Haas (SdH) oscillations and from the Hall resistance. Values of n in our samples were in the range of 0.54 to $7.0 \times 10^{11} \text{ cm}^{-2}$, with a peak mobility of $\mu = 5.1 \text{ m}^2/\text{Vs}$ in sample A1; this is comparable to the highest mobilities reported for Si MOSFETs. Using the AlAs dielectric constant of 10, and the transverse band effective mass $m_b = 0.21$ reported from cyclotron resonance measurements [14], our density range corresponds to $2.8 \leq r_s \leq 9.6$, where r_s is the average inter-electron spacing measured in units of the effective Bohr radius. We made measurements down to $T = 40 \text{ mK}$ using low-frequency lock-in techniques. The samples were mounted on single-axis tilting stages to allow the angle, θ , between the normal to the sample and the magnetic field to be varied from 0° to 90° in situ.

In Fig. 1, we exhibit a characteristic trace of longitudinal resistivity at $\theta = 0^\circ$. The high quality of the sample, as compared to previous 2DESs in narrow AlAs QWs [12], is evident from the persistence of SdH oscillations to fields as low as 0.5 T . The oscillations at the lowest fields correspond to odd-integer Landau level (LL) filling factors (ν), as determined by the ratio of the Zeeman and cyclotron splittings which, in turn, is fixed by the product g^*m^* . A simple analysis reveals that the ν_{xx} minima at odd-integer ν will be strong at the lowest fields when $4j+1 < g^*m^* < 4j+3$, for j a nonnegative integer; this is the case for our 2DES as we will discuss below.

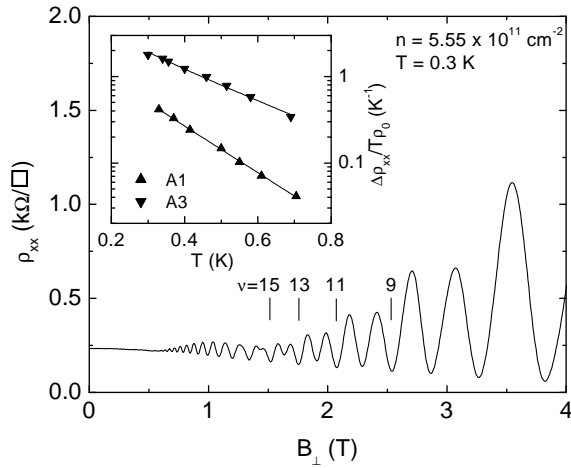


FIG. 1: Longitudinal resistivity (ρ_{xx}) for sample A1 at $n = 5.55 \times 10^{11} \text{ cm}^{-2}$. Inset: Temperature dependence of the amplitude ($\Delta\rho_{xx}$) of SdH oscillations, normalized to the zero-field resistivity (ρ_0), at $B = 1.0 \text{ T}$ for samples A1 (up triangles, $n = 1.82 \times 10^{11} \text{ cm}^{-2}$, $\mu = 4.7 \text{ m}^2/\text{Vs}$) and A3 (down triangles, $n = 1.89 \times 10^{11} \text{ cm}^{-2}$, $\mu = 3.3 \text{ m}^2/\text{Vs}$). The Dingle temperatures give effective masses of 0.45 and 0.30 respectively.

For a quantitative determination of g^*m^* , we measured magnetoresistance in fields applied parallel to the 2DES plane ($\theta = 90^\circ$) to directly observe the total spin polarization field at low densities (Fig. 2), and in tilted fields ($0^\circ < \theta < 90^\circ$) to determine g^*m^* at low fields and high densities (Fig. 3). An example of our parallel field measurements is displayed in Fig. 2. The traces are similar to results from previous experiments [2, 3, 4, 6, 7]: a metallic T -dependence is observed at zero magnetic field, followed by a field-induced transition to an insulating behavior at high fields. There is also a resistance kink whose high field onset, marked by an arrow (B_p) in Fig. 2, signals the total spin polarization of the carriers [2, 6, 15]. In the inset of Fig. 2, we have displayed B_p versus n from our parallel field measurements. By monitoring B_p as n is changed, we can extract g^*m^* as a function of n from the relation $B_p = (2h/e)n/g^*m^*$ (ignoring the possibility of nonlinear spin polarization, which we will address shortly); these g^*m^* are plotted in Fig. 4 (a) (open symbols). The results are normalized by the band values, $g_b = 2$ and $m_b = 0.21$ [11, 14].

In order to augment our determination of g^*m^* at higher densities, we next performed measurements in tilted fields. The quantization of the 2DES energy into LLs depends on the component of the magnetic field perpendicular to the plane of the 2DES, while the Zeeman energy depends on the total field. Thus, by tilting the sample relative to the applied field, we can change the ratio of Zeeman and cyclotron splittings and therefore the strengths of alternating SdH minima [16]. The minima are weakest when a set of spin-down LLs cross a set of spin-up LLs. This corresponds to the condition,

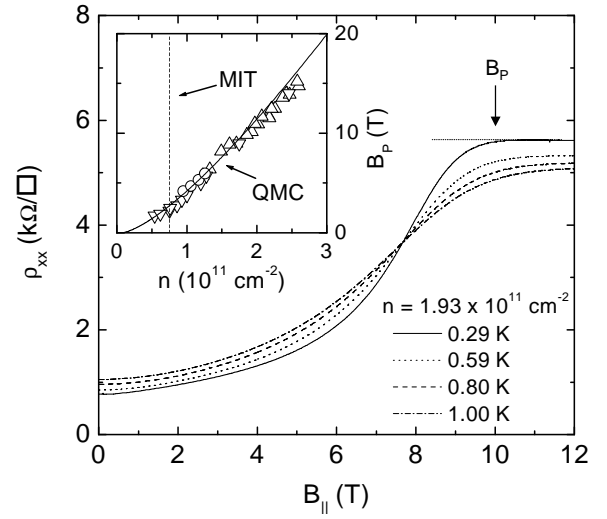


FIG. 2: Parallel-field magnetoresistance at a fixed density for different temperatures. A field-induced transition from metallic to insulating behavior occurs at 7.7 T , and the 2DES becomes fully spin polarized at $B_p = 10.1 \text{ T}$ (indicated by the arrow). Inset: Spin polarization fields (B_p) as a function of density from parallel-field magnetoresistance measurements for samples A1 (up triangles), A3 (down triangles), and B1 (circles). The solid curve represents the quantum Monte Carlo (QMC) prediction for B_p , assuming linear spin polarization with field, and the dotted line indicates the zero-field metal-insulator transition (MIT) observed in our samples.

$1/\cos(\theta_c) = 2i/g^*m^*$, where θ_c is the angle at which the levels cross and i is the difference in LL index between the crossing levels. In Fig. 3 we have plotted, at a fixed density, the strength of SdH minima, ρ_{xx} , for several i as a function of $1/\cos(\theta)$; ρ_{xx} is defined as the average difference between the resistance at a SdH minimum and at the maxima on either side of it. If the minima become indiscernible, such as when a minimum itself becomes a maximum, we simply take $\rho_{xx} = 0$. The LL crossings are indicated by the vertical dashed lines in Fig. 3, with the even-minima experiencing a crossing at $\theta_c = 57.7^\circ$ and the odd-minima at $\theta_c = 74.7^\circ$. The lowest i at which LL crossings are observed is $i = 2$, giving $i = 1$ for the first observed crossing angle. The plot of $1/\cos(\theta_c)$ versus i , shown in Fig. 3 inset, confirms the above LL crossing condition. Using such analysis, we have extracted $g^*m^*/g_b m_b$ versus n and plotted them in Fig. 4 (a) (closed symbols). We note that the values of g^*m^* derived from parallel and tilted field measurements are consistent with each other and with the condition discussed above for the odd-lying SdH minima being strong at low fields.

We now address the linearity of the spin polarization with field. In their study of dilute GaAs 2DESs, Zhu et al. [7] and Tutuc et al. [9] report a significantly nonlinear spin polarization as a function of magnetic field. Measurements by Tutuc et al. [9] demonstrate that the finite

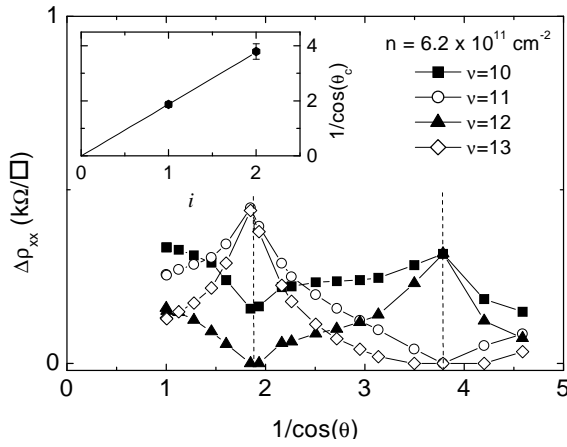


FIG. 3: Strength of SdH m^* in a as a function of tilt angle for several different filling factors. LL crossings are indicated by dashed lines, with the even fillings experiencing a crossing at $\theta_c = 57.7^\circ$ and the odd at 74.7° . The inset shows how the LL crossing angle, θ_c , changes with crossing index, i .

thickness of the electron layer causes an enhancement of the single-particle m^* in parallel field. This enhancement is significant when the magnetic length becomes comparable to or less than the 2DES thickness and accounts for the observed spin polarization nonlinearity in GaAs 2DESs in Ref. [9]. In contrast, we do not expect significant finite-layer thickness effects for a 2DES in narrow AlAs QW given its very small width. Our results indeed reveal no measurable nonlinear spin polarization with magnetic field. First, the LL crossings occur at the same θ_c for all of a given parity (Fig. 3) with only slight deviations at the very lowest θ . Second, the plots of $1/\cos(\theta_c)$ versus i for various densities are all fit well by straight lines that pass through the origin (Fig. 3 inset); this would not be the case if the rate of polarization changed significantly in field. Third, there is good agreement in our values of g^*m^* derived from tilted-field LL crossings and parallel-field B_p measurements, although the former measurement is performed at small, partial spin polarizations and low parallel fields while the latter is done at full polarization and high parallel fields.

Having established the linearity of spin polarization in this system, we compare our B_p and g^*m^* with the prediction of a QMC calculation for an interacting 2DES which has zero thickness and is disorder free [1]. That prediction is drawn as a solid curve in the inset of Fig. 2 and in Fig. 4(a). The agreement of the measured and predicted values is surprisingly good considering that there are no adjustable parameters. For the QMC calculation, we used $m_b = m_t = 0.21$, where the value 0.21 is from the reported cyclotron resonance measurements [14]. We add that we get good agreement between the QMC results and the measured g^*m^* for $0.20 < m_t < 0.23$. This range is also consistent with a recent determination of m_t from ballistic transport measurements in AlAs [18]. On

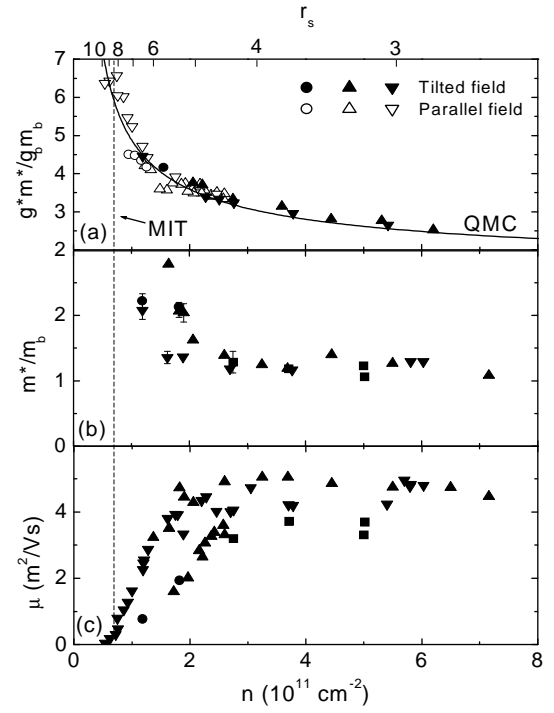


FIG. 4: Shown as a function of density are: (a) spin susceptibility, (b) effective mass, and (c) mobility. In all plots, up triangles correspond to sample A1, squares to A2, down triangles to A3, and circles to B1. The QMC prediction of g^*m^* is included in (a), and the vertical dashed line indicates the density corresponding to the zero-field MIT.

the other hand, SdH measurements of the m^* , including our own, tend to give slightly larger values. As we discuss below, these latter measurements are problematic.

In our samples, we observe a zero-field metal-insulator transition (MIT) at $n = 0.72 \times 10^{11} \text{ cm}^{-2}$ ($r_s = 8.3$), indicated by the vertical dotted line in the inset of Fig. 2 and in Fig. 4. This is close to the value reported for wide AlAs QW with comparable mobilities but with the in-plane valley occupied [19], and SiMO SFETs with two out-of-plane valleys occupied [20]. More importantly, there is no apparent divergence of g^*m^* at the MIT in our samples, and instead the measured g^*m^* coincide with the QMC curve continuously through the transition. The QMC calculation places the ferromagnetic transition in our system at $n = 1 \times 10^{10} \text{ cm}^{-2}$, well below the range accessible in our measurements.

We also performed independent measurements of m^* as a function of n [Fig. 4(b)] by monitoring the T -dependence of the amplitude of low field SdH oscillations and fitting the results with the Dingle formula. Both the mass and the Dingle temperature were allowed to vary as fitting parameters. The masses that we include in Fig. 4(b) at each n were obtained from data taken in the temperature range 0.3 to 0.8 K and fields in the range of 0.50 to 1.5 T. We have included two-sided error bars in Fig. 4(b) to reflect the spread of m^* in this field range. Our

measured m^* at high n are comparable to those reported previously in narrow-well AAs [12, 14]. At low densities, there appears to be some enhancement of m^* that is similar in magnitude to that reported in Si-MOSFETs [5, 10], however there is a significant spread in the m^* values that depends on both sample and cooldown. As examples, in the inset of Fig. 1, we show Dingle plots for two different samples at nearly the same field and density that give markedly different values for m^* . It is noteworthy that the discrepancies become large at approximately the same density where the 2DES mobility begins to drop rapidly [Fig. 4(c)], though there is no direct correlation between the mobilities and m^* values. The Dingle analysis may be producing anomalous results in this system, particularly as the density is reduced, for several reasons. At low densities, the zero-field resistance becomes increasingly T -dependent, complicating the application of the Dingle analysis which presupposes no such dependence. We have tried the analysis employed in Ref. [5] whereby the Dingle temperature is assumed to vary with temperature at the same rate as the zero-field resistance; this fails to appreciably reconcile the discrepancies between the m^* values and simply reduces the overall enhancement at low n . The discrepancies could also be due to inhomogeneities in the 2DES density, which can vary between samples and cooldowns and which would become increasingly significant as the overall density is reduced. In any case, given that the discrepancies observed in m^* are absent in g^*m^* , it appears that the values deduced from the Dingle analysis of the SdH oscillations do not reflect the true m^* at low densities in our samples.

We emphasize that the values of g^*m^* derived from parallel and tilted field measurements are consistent between samples and cooldowns. This is despite differences in mobility, implying that the spin susceptibility is not very sensitive to the effects of disorder. The continued agreement of our measurements with the QMC calculation at low densities, where screening of the disorder potential wanes and the role of disorder becomes more important [Fig. 4(c)], is consistent with this observation.

We have argued that narrow AAs QWs are ideal systems for measuring the role of interaction on the spin susceptibility because of their single-valley occupation, thin electron layer, and isotropic in-plane Fermi contour. We believe these same properties may be responsible for the differences between our results and those in other material systems. Measurements of g^*m^* in Si-MOSFETs generally find less enhancement over the band value than narrow AAs QWs form most of the available range of densities. Initially, this is somewhat surprising considering that (001) Si-MOSFETs have a double-valley occupancy which should produce a more dilute 2DES. However, recent measurements in strain-tunable wide AAs QWs find the same valley occupation dependence of g^*m^* within a single material system, namely less enhancement in the two-valley case [21].

Another system of interest is the dilute GaAs 2DES where the electrons occupy a single, isotropic valley. In Ref. [9], where g^*m^* was determined via B_p measurements, it was shown that the differences between the measured g^*m^* and the QMC results could be essentially reconciled by taking into account the significant Fermi surface distortion that occurs in a thick electron layer system in the presence of a large parallel field. Zhu et al. [7], however, have reported that even in the limit of zero parallel field, the measured g^*m^* remains below the QMC results. While we do not have a firm explanation for this discrepancy, we speculate that the weaker enhancement may be due to an effective reduction of the interaction strength at zero field caused by the very large electron layer thickness in the extremely dilute GaAs 2DESs that were studied in Ref. [7], rendering a system with a smaller effective ϵ_0 than the one calculated assuming zero thickness. A full, quantitative understanding of the differences between the various material systems is still lacking.

We thank the NSF for support, and R. Winkel for discussions. Part of the work was performed at the Florida NHMFL, also supported by the NSF; we thank E. Palm, T. Murphy, and G. Jones for technical assistance.

-
- [1] C. Attaccalite et al, Phys. Rev. Lett. 88, 256601 (2002).
 - [2] T. Okamoto et al, Phys. Rev. Lett. 82, 3875 (1999).
 - [3] S.A. Vitkalov et al, Phys. Rev. Lett. 87, 086401 (2001).
 - [4] A.A. Shashkin et al, Phys. Rev. Lett. 87, 086801 (2001).
 - [5] V.M. Pudalov et al, Phys. Rev. Lett. 88, 196404 (2002).
 - [6] E. Tutuc et al, Phys. Rev. Lett. 88, 036805 (2002).
 - [7] J. Zhu et al, Phys. Rev. Lett. 90, 056805 (2003).
 - [8] O. P. Rus et al, Phys. Rev. B 67, 205407 (2003).
 - [9] E. Tutuc et al, Phys. Rev. B 67, 241309 (2003).
 - [10] A.A. Shashkin et al, Phys. Rev. B 66, 073303 (2002).
 - [11] H.W. van Kesteren et al, Phys. Rev. B 39, 13426 (1989).
 - [12] S. Yamada et al, Physica B 201, 295 (1994); A.F.W. van de Stadt et al, Surf. Sci. 361/362, 521 (1996).
 - [13] The in-plane valleys are occupied when the QW width is $> 55 \text{ \AA}$, so that the strain caused by the lattice mismatch between AAs and the GaAs substrate dominates the valley occupation energies (see Refs. [11, 12]).
 - [14] H. M. Omose et al, Physica E 4, 286 (1999).
 - [15] V.T. Dolgoplov and A. G. Gold, JETP Lett. 71, 27 (2000).
 - [16] F.F. Fang and P.J. Stiles, Phys. Rev. 174, 823 (1968).
 - [17] In the ϵ_0 range accessible in our samples, QMC calculations predict a small nonlinear spin polarization, giving 5% deviations in B_p and g^*m^* (see, e.g., Fig. 4 of Ref. [9]). This is within the error of our measurements, and thus cannot be ruled out. The QMC predictions shown in Figs. 2 and 4 do not include the nonlinearity.
 - [18] O. Gunawan et al, cond-mat/0402265 (2004).
 - [19] S.J. Papadakis and M. Shayegan, Phys. Rev. B 57, R15068 (1998).
 - [20] E. Abraham et al, Rev. Mod. Phys. 73, 251 (2001).
 - [21] Y.P. Shkolnikov et al, cond-mat/0402399 (2004). There are also differences in the g^*m^* enhancement between

narrow and wide AlAs QWs that may be related to the anisotropic in-plane mass of the lattice system.